Nanoscale

Accepted Manuscript

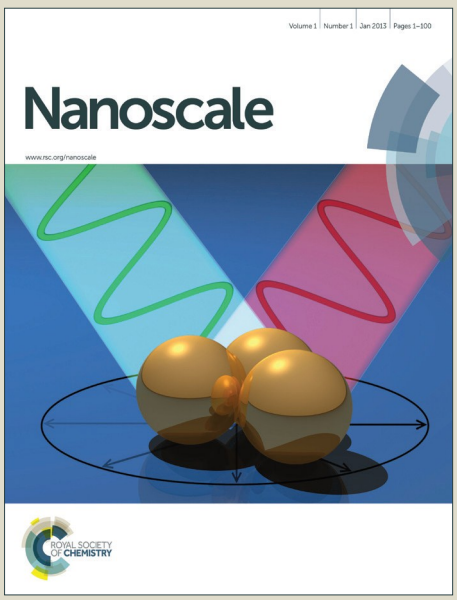

This is an *Accepted Manuscript*, which has been through the Royal Society of Chemistry peer review process and has been accepted for publication.

Accepted Manuscripts are published online shortly after acceptance, before technical editing, formatting and proof reading. Using this free service, authors can make their results available to the community, in citable form, before we publish the edited article. We will replace this *Accepted Manuscript* with the edited and formatted *Advance Article* as soon as it is available.

You can find more information about *Accepted Manuscripts* in the Information for Authors.

Please note that technical editing may introduce minor changes to the text and/or graphics, which may alter content. The journal's standard Terms & Conditions and the Ethical guidelines still apply. In no event shall the Royal Society of Chemistry be held responsible for any errors or omissions in this *Accepted Manuscript* or any consequences arising from the use of any information it contains.

ROYAL SOCIETY OF CHEMISTRY

www.rsc.org/nanoscale

Please do not adjust margins

Journal Name

ARTICLE

Polycatechol Nanosheet: A Superior Nanocarrier for Highly Effective Chemo-Photothermal Synergistic Therapy in Vivo

Received 00th January 20xx,
Accepted 00th January 20xx

DOI: 10.1039/x0xx00000x

www.rsc.org/

J. Bai,[a] X. D. Jia,[a] Z. F. Ma,[a,b] X. E. Jiang,[a,*] and X. P. Sun[c, d, *]

Integration of phototherapy and chemotherapy in a single system holds great promise to improve therapeutic efficiency for tumor but remains a key challenge. In this study, we describe our recent finding that polycatechol nanosheet (PCCNS) can be facilely prepared on a large scale *via* chemical polymerization at 4°C as an effective nanocarrier for loading high-density CuS nanocrystals as photothermal agent. The resulting CuS/PCCNS nanocomposites exhibit good biocompatibility, strong stability, and high photothermal conversion efficiency of ~45.7%. The subsequent loading of anticancer drug doxorubicin (Dox) creates a superior theranostic agent with pH- and heat-responsive drug release, leading to almost complete destruction of mouse cervical tumor under NIR laser irradiation. This development offers an attractive theranostic agent for *in vivo* chemo-photothermal synergistic therapy toward biomedical applications.

Introduction

Cancer is now a leading cause of human death in the world,[1, 2] due possible to the low effectiveness and severe side effects of currently available cancer treatments. The cancer patients treated by conventional approaches such as surgery, radiation therapy, and chemotherapy will suffer from relapses and metastases as well as an increased incidence of the second cancers.[3] Chemo-thermal synergistic therapy has become a potential strategy for cancer treatment with increased therapeutic efficacy,[4] but the traditional heat delivery is usually invasive and nonuniform, and also suffers from sophisticated temperature control.[5] The advent of nanotechnology has presented great opportunities for optimizing the efficacy and operation of chemo-thermal therapy. Some photothermal nanomaterials responsive to near infrared light simultaneously deliver heat and chemotherapeutics to the tumor.[6, 7] The enhanced permeability and retention (EPR) effect of nanomaterials not only increases drug concentration in tumors, but results in the location of the nanomaterial-mediated hyperthermia inside the tumors, thereby greatly improving the specificity and efficacy for cancer treatment.

Till now, a wealth of noble metal nanostructures have been successfully developed as chemo-photothermal agents for tumor therapy, such as gold nanoshells,[8] gold nanorods,[9] hollow gold nanospheres,[10] gold nanocages,[11] and Pd nanosheets.[12] More recently, two-dimensional (2D) nano-materials, like graphene and its derivatives[13, 14] and transition metal dichalcogenides,[15-17] have emerged as attractive nanocarriers for chemo-photothermal agents due to their ultrahigh surface area available for high drug loading on both sides and efficient contact with tumor tissue. However, they all suffer from poor dispersibility in the physiological condition or complex surface modification process. These inevitably hinder the further intracellular utilization of these 2D nanostructures. In addition, the exploration of the single-layer MoS_2 sheet in the area of biomedicine is still in its infancy, mainly suffering from the complicated synthesis process, low yield of single-layer MoS_2, and undesired micrometer sizes. As such, it is highly attractive to design and develop new 2D nanocarriers for highly effective chemo-photothermal synergistic therapy.

Catechols are small molecules widely used in food and pharmaceutical industry. As adhesion molecules, catechols and its derivatives can efficiently and facilely modify almost all organic and/or inorganic surfaces and yield functional surfaces and materials.[18, 19] Therefore, an ever-increasing number of bioinspired catechol-based polymers have received considerable attention in biological field, including dopamine-melanin colloidal nanospheres for *in vivo* cancer therapy.[20] However, relatively little work has been published concerning polycatechol as effective nanocarrier. In this study, we report the development of 2D polycatechol nanosheet (PCCNS) from catechol (CC) monomer by controlling reaction temperature at 4°C (Scheme 1). The 2D PCCNS not only shows photo-thermal property but also can be used as an effective nanocarrier for loading high-density CuS nanocrystals as photo-thermal agent[21-23] and doxorubicin (Dox) as anticancer drug. The as-

[a] State Key Lab of Electroanalytical Chemistry, Changchun Institute of Applied Chemistry, Chinese Academy of Sciences, Changchun 130022, Jilin, China
E-mail: jiangxiue@ciac.ac.cn
[b] Graduate School of the Chinese Academy of Sciences, Beijing 100039, China
[c] College of Chemistry, Sichuan University, Chengdu 610064, Sichuan, China,
E-mail: sunxp@ciac.ac.cn
[d] Chemistry Department & Center of Excellence for Advanced Materials Research, King Abdulaziz University, Jeddah 21589, Saudi Arabia
Electronic Supplementary Information (ESI) available: [The calculation of the photothermal conversion efficiency and supplementary figs. See DOI: 10.1039/x0xx00000x

Nanoscale Accepted Manuscript

Please do not adjust margins

obtained CuS/PCCNS-Dox nanocomposites cause almost complete destruction of cervical cancer in mouse model under near infrared (NIR) laser irradiation. Thus, it offers us a superior theranostic agent for *in vivo* chemo-photothermal synergistic therapy.

Experimental

Materials

Catechol was purchased from Alfa Aesar. Doxorubicin hydrochloride (Dox) was purchased from Beijing Huafeng United Technology Co. Dimethyl sulfoxide (DMSO), 3-(4,5-dimethylthiazol-2-yl)-2,5-dipheny-ltetrazolium bromide (MTT) were purchased from Sigma-Aldrich. Dulbecco's modified eagle medium (DMEM), penicillin, fetal bovine serum (FBS), and streptomycin were purchased from Beijing Dingguo Biotechnology Co. Other chemicals were of analytical grade and used as received without further purification. Phosphate buffered saline (PBS) used in cell culture, was purchased from Invitrogen (10010). In all experiments, deionized water was used.

Characterization

TEM was performed using a H-600 electron microscope (Hitachi, Japan) operated at 75 keV. TEM samples were prepared by depositing a diluted suspension of nanocomposites onto a carbon-coated copper grid and air dried before the measurements. AFM images were taken with a Multimode-V atomic force microscope, operating in tapping mode in air. The optical properties of nanomaterials were characterized using an UV-vis spectrometer (Lambda 25, Perkin-Elmer, USA) with a 1 cm cuvette. FT-IR spectra were recorded on a Nicolet 6700 FT-IR spectrometer with KBr pellets in the 4000–500 cm^{-1} region. Raman spectra were obtained on a J-Y T64000 Raman spectrometer with a 514.5 nm wavelength incident laser light. The cells images were recorded using confocal laser scanning fluorescence microscope (CLSM, Leica TCS SP2, Leica Microsystems, Mannheim, Germany). *In vitro* cytotoxicity was measured using a Versamax microplate reader (Bio-Tek Instruments, Inc., Winooski, VT, USA).

Synthesis of PCCNS

In a typical procedure, 2.0 g of catechol was added to a mixed solution of $NH_3 \bullet H_2O$ (2 mL) and water (30 mL) at 4°C under vigorous stirring for 24 h. A series of color changes from colorless to light yellow, brown and then dark brown were observed, indicating the formation of PCCNS. Then PCCNS was cracked by ultrasonic probe at 200 W for 2h in order to obtain small size PCCNS, which facilitates cellular entry and dispersion stability, and is more suitable for biological systems.

Synthesis of CuS/PCCNS Nanocomposites

In a typical synthesis, 10 mL of $CuCl_2 \bullet 5H_2O$ aqueous solution (1 mM) was added into 1 mL of PCCNS aqueous suspension (1.0 mg/mL) under stirring at room temperature, and kept the magnetic stirring for 30 min. After gentle mixing of the solution, 100 μL of Na_2S aqueous solution (0.1 M) was added into the reaction solution with continuous stirring. After 10 min, the mixture was heated to 90°C for 15 min until a dark solution was obtained. After reaction, the resultant mixture was purified by centrifugation and water-washing for several times. The products were designated as CuS/PCCNS.

Photothermal Heating Measurements

The test solution was suspended in a quartz cuvette, irradiated by the 980 nm laser (Changchun New Industries Optoelectronics Technology, China) with a power density of 1.0 W/cm^2 for 10 min. The solution temperature was monitored by a digital thermometer (Pyrometer Instrument Company, USA). For detecting the photostability of CuS/PCCNS nanocomposites, the samples were irradiated with 980 nm NIR laser for 10 min (laser on), followed by naturally cooling to room temperature without NIR laser irradiation for 30 min (laser off). This cycle was repeated for five times.

Drug Loading on and Release from CuS/PCCNS Nanocomposites

Dox loading onto CuS/PCCNS nanocomposites was done by simply mixing Dox with CuS/PCCNS solution at pH 8.0 and the mixture was stirred in the dark for 24 h. Next, residual Dox molecules were removed by centrifugation and thoroughly washed with PBS until the supernatant became free of reddish color. Finally, the CuS/PCCNS-Dox nanocomposites were re-suspended and stored at 4°C. To evaluate the Dox-loading efficiency (DLE), the residual Dox content (R_{Dox}) was determined by UV-vis measurements at a wavelength of 490 nm. The DLE can be calculated as follows: $DLE\% = [(O_{Dox} - R_{Dox})/O_{Dox}] \times 100\%$, in which O_{Dox} and R_{Dox} is the original and residual Dox content, respectively.

For the *in vitro* release experiment, the above-prepared CuS/PCCNS-Dox nanocomposites were immersed in 2 mL of PBS (pH 5.5, 7.4 and 9.0) at 37°C and shaken at 100 rpm. At certain time intervals, aliquots of PBS (2 mL) were taken out by centrifugation to test the concentration of released Dox and replaced with 2 mL of fresh buffer solution. The concentration of Dox released from CuS/PCCNS-Dox into PBS was quantified using UV-vis spectroscopy.

Cell Culture

HeLa cells (cervical cancer cell line) were cultured in a DMEM medium and supplemented with 10% fetal bovine serum, 100 units mL^{-1} penicillin and 100 mg mL^{-1} streptomycin at 37°C in a humidified 5% CO_2 atmosphere. The media were changed every two days. For all experiments, cells were harvested from subconfluent cultures by the use of trypsin and were re-suspended in fresh complete medium before plating.

***In Vitro* Cytotoxicity Study**

For cytotoxicity assay, HeLa cells were cultured in 96-well plate with 100 μL of media at a density of 1×10^4 cells/well for 24 h prior to assay. After the cells were washed, the different concentrations of CuS/PCCNS were added into the wells, and the cells were incubated in 5% CO_2 at 37°C for 24 h. To assess the therapeutic effect of CuS/PCCNS-Dox, free Dox (10 μg/mL), CuS/PCCNS (640 μg/mL), and CuS/PCCNS-Dox (640 μg/mL, the concentration of Dox was 10 μg/mL) were added to the medium, and the cells were incubated for 24 h. For

Nanoscale Accepted Manuscript

This journal is © The Royal Society of Chemistry 20xx

photothermal therapy, corresponding wells were irradiated with a 980 nm NIR laser (1.0 W/cm^2) for 5 min. After the incubation, the culture medium with nanoparticles was removed and washed three times with PBS. 100 μL of MTT solution (0.5 mg/mL) was added to each well, and then the mixture was incubated for another 4 h. Finally, the medium was replaced with 100 μL of DMSO. The absorbance was monitored at 570 nm using a Versamax microplate reader (BioTek Instruments Inc, USA). Results were quantified by manually subtracting the blank value and normalized against the control values.

Confocal Fluorescence Imaging Analysis

Prior to confocal microscopy study, HeLa cells were plated onto glass bottom cell culture dishes (20 mm) at a density of 5.0×10^5 cells per dish at 37°C in a humidified atmosphere containing 5% CO_2 for 24 h. The cells were washed three times with PBS, followed by incubation with 800 μL of CuS/PCCNS (640 μg/mL) and CuS/PCCNS-Dox (640 μg/mL, the concentration of Dox was 10 μg/mL) solution in DMEM medium at 37°C for 24 h. For photothermal therapy, corresponding culture dishes were irradiated with a 980 nm NIR laser (1.0 W/cm^2) for 5 min. Finally, the solution was removed and the cells were washed three times with PBS (pH 7.4) and stained with 2 μg/mL of calcein AM in PBS for 30 min. The cells were visualized under a confocal laser scanning fluorescence microscope with 10×objective. The dye was excited at 488 nm and observed through a 500-550 nm emission band-pass.

***In Vivo* Chemo-Photothermal Destruction of Tumors**

Kuming mice were obtained from Animal Experimental Center of Jilin University. All experiments were performed in compliance with the relevant laws and institutional guidelines, and approved by the Animal Care Committee of Jilin University. The mice were inoculated subcutaneously with 5×10^6 U14 cells in the left forelimb armpit before the experiment. When the tumor volume reached ~50 mm^3, the mice were randomly divided into 4 groups, and saline solution (Group I, 0.9%), free Dox (Group II, 10.0 μg/mL), CuS/PCCNS (Group III, 640 μg/mL) and CuS/PCCNS-Dox (Group IV, 640 μg/mL, and the concentration of Dox was 10.0 μg/mL) were locally injected into the tumors. Mice in group III and IV received intratumorally injections of 640 μg/mL CuS/PCCNS (0.1 mL) and 640 μg/mL CuS/PCCNS-Dox (0.1 mL), and were followed by NIR irradiation (1.0 W/cm^2, 5 min) after each drug injection. Then the tumor size dimensions were measured with a caliper every three days, and the tumor volumes were calculated according to the equation: Volume = (Tumor Length) × (Tumor Width)^2/2. At 19th day, all the animals were euthanized, and the tumors were dissected and weighed to evaluate the therapeutic efficacy of the different groups.

Biodistribution of Nanoparticles in Mice

To quantitatively assess the biodistribution of CuS/PCCNS nanocomposites, tumor-bearing mice were treated by intratumoral injection with 200 μL of CuS/PCCNS nanocomposite solution. The mice were sacrificed at 24 h post-injection, and main tissues (heart, liver, spleen, lung, kidney and tumor) were collected for inductively coupled plasma mass spectrometry (ICP-MS) analysis.

For ICP-MS analysis, the tissue samples were further treated with 5.0 mL of aqua regia (HCl:HNO_3=3:1) overnight. After all the tissues were digested in the solutions, the samples were diluted in 10 mL aqua regia and the concentrations of Cu were measured using ICP-MS.

Histology Analysis

After 19 days, all the animals were sacrificed, and the tumors were excised for histopathologic analysis. The tissue was fixed in 4% neutral buffered formalin and processed routinely into paraffin. The sliced tumors of 4 μm thickness were stained with hematoxylin & eosin (H&E) and observed by a digital microscope (Leica QWin).

Results and discussion

Preparation and Characterization of 2D PCCNS and CuS/PCCNS

The PCCNS was synthesized for the first time through the oxidation and self-polymerization method from the precursor of catechol (CC) in the mixture of water and ammonia monohydrate (NH_3•H_2O) at 4°C. The freshly-made mixture solution gradually changed in color from colorless to deep brown at 4°C (Fig. S1) and the resulting dispersion shows an additional UV-vis absorption peak at 338 nm (Fig. S2, curve b) with significant decrease of the absorption peak at 277 nm for CC monomer (Fig. S2, curve a).[24] To evaluate the structural properties of polycatechol, corresponding fourier transform infrared (FTIR) spectra were taken as shown in Fig. 1A. By comparing spectra, a remarkable feature is that the number of absorption peaks of polycatechol is much less than that of catechol. This is a general feature for polymerization of a monomer. The monomer shows the doublet peaks at 3450 and 3324 cm^{-1} that belong to characteristic hydrogen-bonded phenolic O-H vibration bands, and C=C stretching vibrations of benzene ring at 1623 and 1514 cm^{-1},[25] while the ν_{OH} peak at 3324 cm^{-1} disappears in the spectrum of polycatechol. This indicates that the polymerization of catechol may be carried out by eliminating one of the two O-H bonds in catechol and retaining another one in polycatechol. The peaks at 1232 and 1425 cm^{-1} in the spectrum of polycatechol may be attributed to the asymmetriocal stretching vibration of C-O-C and substituted benzene ring vibrations. This indicates that a C-O-C bond is contained in the polymer. The broad phenolic O–H

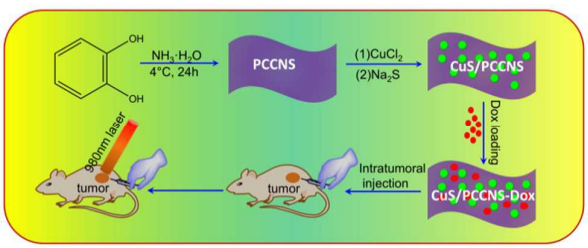

Scheme 1. Preparation of 2D PCCNS and used as a novel nanocarrier for loading CuS nanocrystals and Dox drug for in vivo chemo-photothermal synergistic therapy.

Nanoscale Accepted Manuscript

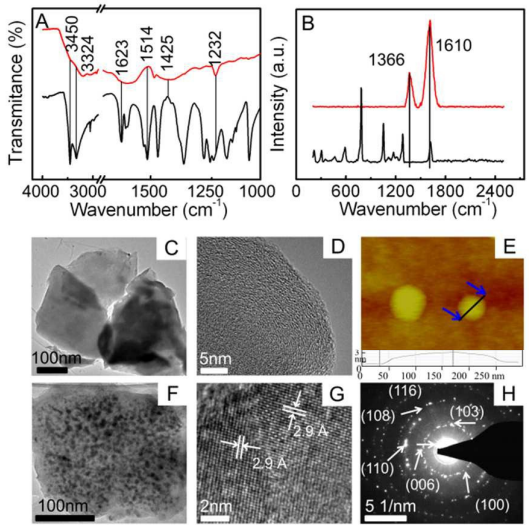

Fig. 1 Characterization of nanomaterials. FTIR spectra (A) and Raman spectra (B) of CC (black line) and PCCNS (red line). (C), (D) TEM images of PCCNS. (E) AFM images of PCCNS. (F) TEM image of CuS/PCCNS nanocomposites. (G) HRTEM image and (H) SAED pattern taken from the CuS nanoparticles.

adsorption band at 3450 cm^{-1} and intense phenyl ether bond absorption at 1232 cm^{-1} in the polycatechol indicate that the polymerization of catechol eliminates one O-H group in catechol to form a C-O-C bond. All these observations support the formation of a higher molecular weight polymer. Also, Raman spectra were used to determine the structure of polycatechol. As shown in Fig. 1B, the Raman spectrum of catechol monomer exhibits several sharp peaks (black line). However, the spectrum of polycatechol has only two bands at 1366 and 1610 cm^{-1} (red line), corresponding to the multi-ring deformation vibrations and the vibration of phenyl ring deformation. The intensified peak at 1610 cm^{-1} and the appearance of peak at 1366 cm^{-1} after polymerization are the characteristic of polymerization of catechol. Based on the FTIR and Raman spectra, we could infer that the polymerization of catechol proceeds via head-to-tail coupling similar to the polymerization of phenol and phenol derivatives (Fig. 2).

Fig. 1C and D show typical transmission electron microscopy (TEM) images of PCCNS, indicating its 2D nature with a mean diameter of about 220 nm. Atomic force microscopy (AFM) analysis reveals that such nanosheet is about 3.1 nm in thickness (Fig. 1E), implying its ultrathin nature. We should point out that a higher reaction temperature like 10°C gives PCCNS with PCC nanospheres, while only gives PCC nanospheres at 30°C with an average size of ~35 nm (Fig. S3), a similar morphology of dopamine-melanin nanospheres as observed by Liu et al,[20] suggesting lower reaction temperature is the key to nanosheet formation although the exact mechanism is not clear at present time. Given catechol and dopamine share almost similar chemical structure, it is thus reasonable to conclude that an oxidation and self-polymerization process is also involved in the formation of PCCNS.[20] As previous reports,[26] it is possible to vary the rate of free radical generation by changing reaction

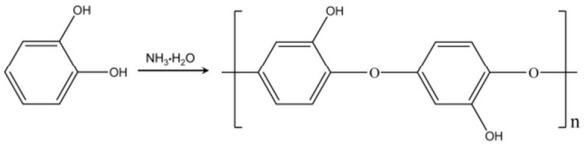

Fig. 2 The proposed chemical structure of polycatechol nanosheet.

temperature. The low levels of free radical and slow polymerization rate might be conducive to the growth of the polymer chain at low temperature, and form large sheet-shaped polymer, while at higher temperatures, the number of instantaneous nucleation is greater, which might lead to decline of precursor stages concentration, and favour the formation of small-sized nanospheres.

The oxygen-containing functional groups of the surface of PCCNS not only endow the nanomaterials with excellent dispersibility and stability in water but also provide a large amount of anchoring sites and facilitate the binding of positive charged copper ions (Cu^{2+}). The copper (II)-loaded PCCNS was subsequently treated with sodium sulfide dissolved in a water, resulting in the formation of CuS/PCCNS nanocomposites. Fig. 1F shows the TEM image of CuS-loaded PCCNS, revealing the PCCNS nanosheet is uniformly decorated by high-density CuS nanoparticles with an average diameter of 10 nm, which should be attributed to the oxygen-containing functional groups uniformly existing on the two accessible sides of PCCNS with a more negative zeta potential (-25.6 mV). The CuS nanoparticles are highly crystalline with d-spacing of 2.9 Å corresponding to the {006} planes of covellite type CuS (Fig. 1G). The diffraction rings in the selected area electron diffraction (SAED) pattern can be indexed to the (100), (103), (006), (110), (108) and (116) planes of covellite CuS, as shown in Fig. 1H. In addition, the CuS/PCCNS nanocomposites show a broad absorption band at 983 nm, providing another piece of clear evidence to support the successful loading of CuS nanostructures (Fig. S2, curve c).[27] It is important to point out that both PCCNS and CuS/PCCNS exhibit excellent dispersibility (Fig. S1) and can be very stable for several weeks without the observation of any floating or precipitated particles.

Photothermal Conversion and *In Vitro* Dox Delivery of CuS/PCCNS Nanocomposites

The powerful optical absorbance of CuS/PCCNS nanocomposites in the near-IR region means a potential for their photothermal conversion upon a 980 nm laser irradiation. To evaluate its photothermal effect, the CuS/PCCNS dispersion was exposed to a 980 nm laser at a power density of 1.0 W/cm^2 for 10 min, and pure water and PCCNS suspension were used as controls (Fig. 3A). The temperature of CuS/PCCNS suspension increases to 51.8°C. In comparison, the temperature of PCCNS suspension and pure water only increases to 40.8°C and 31°C, respectively. It is even unaffected after five cycles of laser on/off irradiation (Fig. 3B). Moreover, the laser irradiation does not change the absorption spectrum of CuS/PCCNS dispersion (Fig. S4), suggesting the good photo-thermal stability of CuS/PCCNS. The

Nanoscale Accepted Manuscript

This journal is © The Royal Society of Chemistry 20xx

Please do not adjust margins

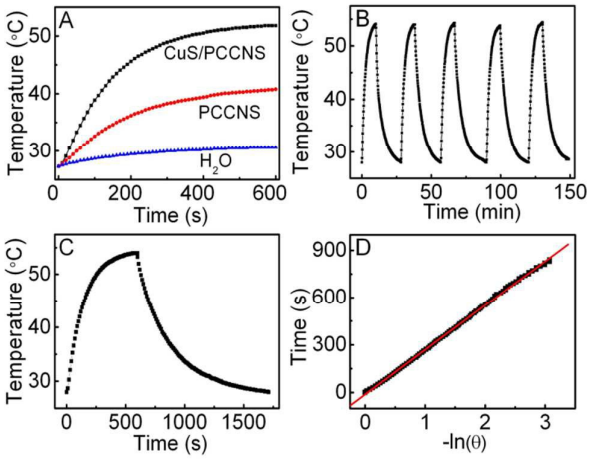

Fig. 3 Evaluation of photothermal property of CuS/PCCNS. (A) Temperature elevation of nanocomposites dispersed in 1 mL of water solution over a period of 10 min under NIR light irradiation (980 nm, 1 W/cm^2 at 1 mg/mL with water as a control. (B) Temperature elevation of CuS/PCCNS nanocomposites dispersed in 1 mL of water solution (1 mg/mL) over five laser on/off cycles under NIR laser irradiation. (C) The photothermal response of CuS/PCCNS aqueous solution (1 mg/mL) for 600 s with an NIR laser (980 nm, 1 W/cm^2) and then the laser was shut off. (D) Linear time data versus −lnθ obtained from the cooling period of Fig. 2C.

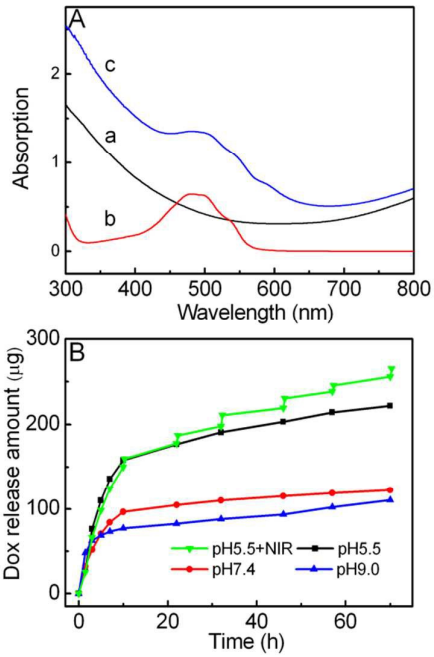

Fig. 4 *In vitro* Dox delivery of CuS/PCCNS nanocomposites. (A) UV–vis absorption spectra of CuS/PCCNS (a), free Dox (b) and CuS/PCCNS-Dox nanocomposites (c) dispersed in PBS. (B) The release of Dox from CuS/PCCNS at pH 5.5 with and without NIR irradiation, at pH 7.4 and pH 9.0.

photo-thermal conversion efficiency (η) for this nanocomposites is calculated as ~45.7% from Fig. 3C and D (Supporting Information),[28] much higher than that of mostly used Au nanorods (22%),[20] promising its use as an attractive photo-thermal agent.

Another unique feature of CuS/PCCNS nanocomposites lies in the large surface area of PCCNS, providing an ideal nanocarrier to load drugs for tumor treatment. Thus, Dox as a model drug was loaded onto CuS/PCCNS to obtain CuS/PCCNS-Dox nanocomposites. The resulting composites show a characteristic peak of Dox absorbance at 490 nm (Fig. 4A). Also, the loading efficiency of Dox on CuS/PCCNS nanocomposites was calculated by measuring the concentration of unbound drug according to the characteristic absorption of free Dox in the UV-vis spectra (Fig. S5). The drug loading capacity of CuS/PCCNS nanocomposites for Dox can reach 850 μg in the total drug concentration of 1.0 mg and the drug loading content was 425 μg Dox per 1.0 mg CuS/PCCNS nnaocomposites, which is far beyond the common drug carrier materials,[29, 30] implying the promising potential of PCCNS as drug delivery agent. The interaction between the PCCNS and Dox is possible due to π–π stacking and hydrophobic interaction, similar to that with GO, but PCCNS is advantageous in terms of its low cost and facile preparation. More importantly, the CuS/PCCNS-Dox still shows excellent water dispersibility (Fig. S6) with pH-dependent drug release property (Fig. 4B). After 70 h, the cumulative amount of released Dox could reach up to 221 μg at pH 5.0, which is obviously higher than 122 μg and 110 μg at pH 7.4 and 9.0. The higher Dox release amount of the CuS/PCCNS-Dox nanocomposites at acidic condition should be mainly attributed to the protonated amine (-NH_2) groups of Dox at low pH, resulting in enhanced Dox water solubility and decreased π–π or hydrophobic interaction between Dox and PCCNS. Obviously, the enhanced drug release under acidic conditions will be favourable for tumor therapy. NIR laser irradiation further enhances the Dox release from CuS/PCCNS-Dox nanocomposites at pH 5.5. During the Dox release process, 10 min NIR laser irradiations (980 nm, 1.0 W/cm^2) were given at different time points. As shown in Fig. 4B, after 10 min NIR irradiation at 10 h, the cumulative amount of released Dox was increased from 149 μg to 159 μg. When the NIR laser was switched off, the release rate was significantly reduced. Similar results were also observed when the laser irradiation was repeated beginning at 22 h, 32 h, 46 h, 57 h and 70 h. The results suggest that the NIR light can enhance the Dox release from the nanocomposites. The reason is that heat stimulates dissociation of the strong interactions between Dox and PCCNS including π–π stacking, and quickly accelerates the release of Dox from the CuS/PCCNS nanocomposites.[31] To further verify this, the release of drug from the CuS/PCCNS nanocomposites was conducted in a water bath at 37°C and 45°C (Fig. S7). Approximately 247 μg of Dox was released at 45°C, which is higher than that at 37°C (202 μg). The release rate of Dox was accelerated by heat, which is similar to the case of laser irradiation. The pH-sensitive and NIR-stimulative Dox release profiles endow the CuS/PCCNS-Dox nanocomposites with on-demand drug release ability, which will effectively avoid the side effect of thermo-chemotherapy.

***In Vitro* Cytotoxicity Study**

Biocompatibility is a critical factor for the biomedical applications of nanoparticles. To evaluate the potential of CuS/PCCNS in biomedicine, its cytotoxicity was studied on HeLa cells through standard 3-(4,5-dimethylthiazol-2-yl)-2,5-

Nanoscale Accepted Manuscript

Please do not adjust margins

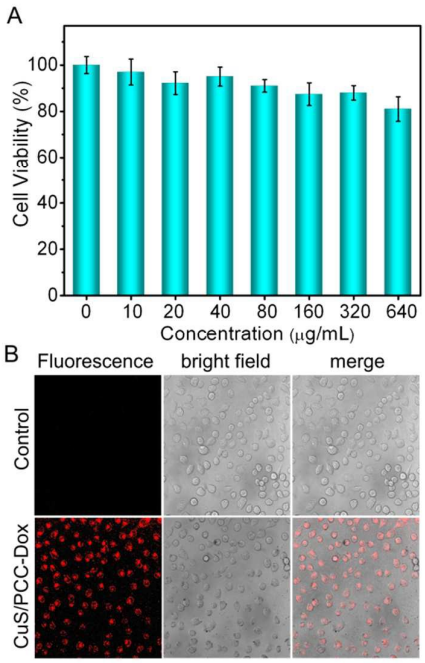

Fig. 5 (A) The viabilities of HeLa cells incubated with different concentrations of CuS/PCCNS for 24 h. (B) Confocal fluorescence images of HeLa cells treated without and with CuS/PCCNS-Dox nanocomposites.

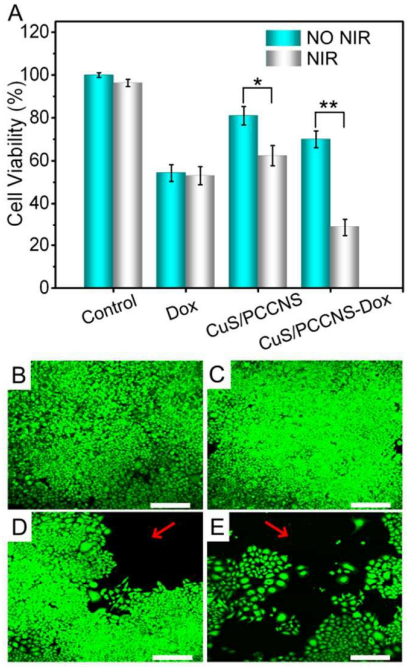

Fig. 6 *In vitro* therapeutic effect evaluation of the nanocomposites. (A) Cell viabilities of HeLa cells incubated with DMEM as control, free Dox, CuS/PCCNS and CuS/PCCNS-Dox nanocomposites with (light gray) and without (cyan) NIR irradiation. Error bars were collected based on the standard deviations (STDEV) of six parallel samples. P values were calculated by the methodology of Student's t test (*p<0.05, **p<0.01, or ***p<0.001). CLSM of Calcein AM stained HeLa cells incubated with (B) DMEM medium, (C) CuS/PCCNS nanocomposites without irradiation and (D) CuS/PCCNS and (E) CuS/PCCNS-Dox nanocomposites with 5 min NIR irradiation. Red arrow indicates the laser spot. Scale bar = 300 μm.

diphenyltetrazolium bromide (MTT) assay (Fig. 5A). Over a wide concentration range from 0 to 320 μg/mL, ~90% of HeLa cells remained viable, and even concentration up to 640 μg/mL, more than 83% cells remained viable, suggesting the good biocompatibility of CuS/PCCNS nanocomposites and the basis for *in vivo* cancer therapy (Fig. 5A). To investigate the internalization and drug delivery ability of CuS/PCCNS nanocomposites, Dox was loaded onto the CuS/PCCNS and incubated with HeLa cells. After 4h incubation, obvious red fluorescence of Dox can be observed from HeLa cells treated with CuS/PCCNS-Dox compared with very weak fluorescence in control group (Fig. 5B), indicating that Dox can be successfully delivered into the cells through CuS/PCCNS nanocomposites.

Furthermore, the *in vitro* therapeutic effect of CuS/PCCNS nanocomposites was also studied with MTT assay (Fig. 6A). NIR laser irradiation has no significant effect on cell viability when the cells treated with DMEM or Dox compared with unirradiated cells, indicating the laser irradiation itself cannot bring distinct damage to living cells. Also the CuS/PCCNS nanocomposites without laser irradiation result in 19% cell inhibition rate at the concentration of 640 μg/mL, which is slightly higher cytotoxicity than the results in Fig. 5A but still comparable. However, in the presence of laser irradiation, CuS/PCCNS nanocomposites show higher cytotoxicity compared to unirradiated cells, suggesting that the heat generated from the NIR irradiation could kill partial cells. Such difference is further enlarged in the presence of CuS/PCCNS-Dox nanocomposites due to the synergistic effect of the chemotherapy of Dox and photothermal therapy of CuS/PCCNS. Nearly 71.3% of cells were killed by the CuS/PCCNS-Dox nanocomposites under 5 min NIR irradiation at an equivalent Dox concentration of 10μg/mL. Notably, the biocompatibility of the CuS/PCCNS-Dox nanocomposites is obviously high without NIR irradiation compared with the free drug at the same concentration since the inhibition rate is only 30%, possibly due to delayed Dox release from CuS/NPCC-Dox nanocomposites.

The *in vitro* therapeutic effect of CuS/PCCNS-Dox nanocomposites was also confirmed by confocal laser scanning microscope (CLSM) measurements. The cells treated with CuS/PCCNS nanocomposites only show negligible cell death compared with negative control group (Fig. 6B and C). However, in the presence of CuS/PCCNS under NIR irradiation, HeLa cells show apparent death within the laser spot (Fig. 6D), suggesting that CuS/PCCNS nanocomposites can mediate the photothermal destruction of HeLa cells. Notably, the cell death area expands beyond the spot of the laser irradiation when the HeLa cells were incubated with CuS/PCCNS-Dox nanocomposites following the NIR laser irradiation (Fig. 6E) due to the release of Dox under irradiation. These results further suggest that CuS/PCCNS-Dox can effectively kill the cancer cells through a synergistic chemo-photothermal therapy.

***In Vivo* Chemo-Photothermal Therapy**

To assess their *in vivo* therapeutic potential, the CuS/PCCNS-Dox nanocomposites were used to treat U14 cervical cancer in

Nanoscale Accepted Manuscript

This journal is © The Royal Society of Chemistry 20xx

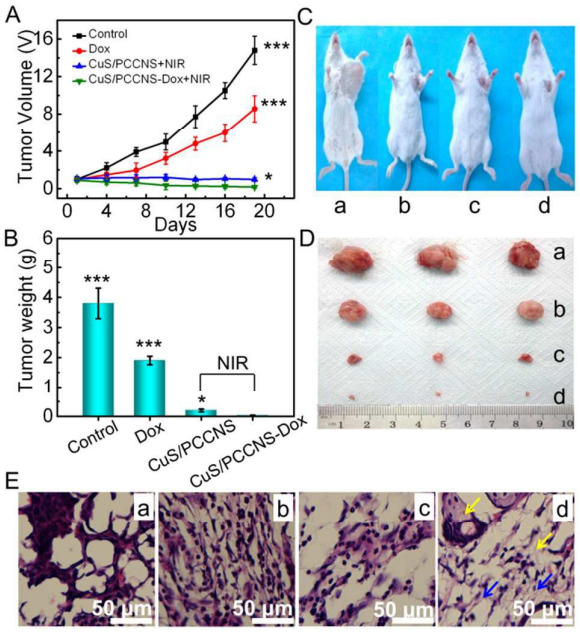

Fig. 7 *In vivo* evaluation of chem-photothermal therapeutic effect. (A) Relative tumor volume of different groups after treatment. (B) Mean tumor weights. Representative photo-graphs of the test mice (C) and tumors from the control group (a), Dox group (b), CuS/PCCNS+NIR group (c), and CuS/PCCNS-Dox+NIR group (D). (E) H&E staining of the tu-mor tissue sections after treatment with saline (a), free Dox (b), CuS/PCCNS+NIR (c) and CuS/PCCNS-Dox+NIR (d). P values were calculated by the methodology of Student's t test (*p<0.05, **p<0.01, or ***p<0.001).

Kunming mice (Fig. 7). Four groups of U14 tumor-bearing mice were tested in this study by intratumoral injections using following agent: saline solution as negative control (group I), free Dox at the concentration of 10 μg/mL (group II), CuS/PCCNS with laser irradiation (group III), and CuS/PCCNS-Dox with laser irradiation (group IV). To examine the kinetic of tumor growth, the tumor volumes were monitored using a caliper before each injection and then calculated (Fig. 7A). The growth of tumor on mice treated with CuS/PCCNS nanocomposites and NIR laser irradiation was effectively inhibited during the observed time (Fig. 7A), while the tumors received chemotherapy alone were not significantly inhibited. Notably, the tumors treated with CuS/PCCNS-Dox nanocomposites and NIR laser irradiation were almost completely destructed. After 19 days of observation, tumors were taken out for weighing and photographing (Fig. 7B and D). The average weights of the tumors for these mice were about 3.8, 1.9, 0.2, and 0.03 g for control group, Dox group, CuS/PCCNS+NIR group, and CuS/PCCNS-Dox+NIR group, respectively (Fig. 7B). The weight of tumors of the CuS/PCCNS-Dox+NIR group was much lighter than that of the other groups. At the same time, the tumor tissue sections were stained by haematoxylin and eosin (H&E) in Fig. 7E. The cytoplasm was stained in pink by aqueous solution of eosin Y and the nucleus was stained in purple by hematoxylin. Extensive nuclear pyknosis, karyolysis, coagulative necrosis and large area of cytoplasm stained red can be observed in histological sections from tumor tissue treated with CuS/PCCNS-Dox and NIR laser irradiation (Fig. 7E, d), indicating the effective destruction of tumor cells. While group treated with saline solution shows no obvious cell apoptosis (Fig. 7E, a). The groups treated with free Dox (Fig. 7E, b) and CuS/PCCNS (Fig. 7E, c) with NIR irradiation show large areas of neoplastic cells with nuclear atypia, revealing insufficient damage to the tumors. Our results confirm the superior antitumor efficacy of CuS/PCCNS-Dox *in vivo*.

We also evaluated the impact of intratumoral injection on the biodistribution of CuS/PCCNS nanocomposites. Biodistribution data was obtained at 24 h after intratumoral injection of CuS/PCCNS, and major organs of mice were severally collected and solubilized with aqua regia ($HCl:HNO_3$=3:1) for ICP-MS measurement of Cu. Fig. S8 shows that, on intratumoral injection, the highest amounts of Cu concentrations were always detected in the tumor, followed by the spleen and liver, which are reticuloendothelial systems (RES) and responsible for the clearance of foreign nanoparticles by macrophage uptake. These findings indicate that, in addition to increasing the tumor concentrations of nanocomposites, intratumoral injection also decreases its localization to healthy tissues.

Conclusions

In summary, polycatechol nanosheets have been facilely prepared *via* low-temperature chemical polymerization of catechol monomers under basic condition. This 2D PCCNS behaves as a superior nanocarrier for loading CuS and Dox and the resulting composites demonstrate high photothermal conversion efficiency, excellent dispersibility and stability in water, NIR photostability, and on-demand drug release profile in response to low pH and NIR laser. It can efficiently kill cancer cells upon NIR laser irradiation. This study not only highlights the utilization of PCCNS as an easily-made nanocarrier for highly effective chemo-photothermal synergistic therapy, but would open exciting new avenue to explore the design of PCCNS-based bio-hybrids for other biomedical applications.

Acknowledgements

This work was financially supported by the National Science Foundation for Excellent Young Scholar of China (21322510), Science and Technology Innovation Foundation of Jilin Province for Talents Cultivation (Grants 20150519014JH), the Youth Foundation of China (21505130), and Youth Foundation of Jilin Province (20140520082JH).

Notes and references

1 A. Jemal, R. Siegel, E. Ward, T. Murray, J. Xu, C. Smigal and M. J. Thun, *CA Cancer J. Clin.*, 2006, **56**, 106.
2 R. Bardhan, S. Lal, A. Joshi and N. J. Halas, *Acc. Chem. Res.*, 2011, **44**, 936.

Nanoscale Accepted Manuscript

3 P. G. Morris and A. B. Lassman, *Nat. Rev. Clin. Oncol.*, 2010, **7**, 428.
4 J. P. May and S.-D. Li, *Expert Opin. Drug Delivery*, 2013, **10**, 511.
5 D. K. Chatterjee, P. Diagaradjane and S. Krishnan, *Ther. Delivery*, 2011, **2**, 1001.
6 A. Agarwal, M. A. Mackey, M. A. El-Sayed and R. V. Bellamkonda, *ACS Nano*, 2011, **5**, 4919.
7 L. Tong, Y. Zhao, T. B. Huff, M. N. Hansen, A. Wei and J. X. Cheng, *Adv. Mater.*, 2007, **19**, 3136.
8 H. Liu, D. Chen, L. Li, T. Liu, L. Tan, X. Wu and F. Tang, *Angew. Chem. Int. Ed.*, 2011, **50**, 891.
9 C. Wang, J. Chen, T. Talavage and J. Irudayaraj, *Angew. Chem. Int. Ed.*, 2009, **48**, 2759.
10 W. Lu, M. P. Melancon, C. Xiong, Q. Huang, A. Elliott, S. Song, R. Zhang, L. G. Flores, J. G. Gelovani, L. V. Wang, G. Ku, R. J. Stafford and C. Li, *Cancer Res.*, 2011, **71**, 6116.
11 L. Gao, J. Fei, J. Zhao, H. Li, Y. Cui and J. Li, *ACS Nano*, 2012, **6**, 8030.
12 W. Fang, S. Tang, P. Liu, X. Fang, J. Gong and N. Zheng, *Small*, 2012, **8**, 3816.
13 K. Yang, S. Zhang, G. Zhang, X. Sun, S. T. Lee and Z. Liu, *Nano Lett.*, 2010, **10**, 3318.
14 J. T. Robinson, S. M. Tabakman, Y. Liang, H. Wang, H. Sanchez Casalongue, D. Vinh and H. Dai, *J. Am. Chem. Soc.*, 2011, **133**, 6825.
15 S. S. Chou, B. Kaehr, J. Kim, B. M. Foley, M. De, P. E. Hopkins, J. Huang, C. J. Brinker and V. P. Dravid, *Angew. Chem. Int. Ed.*, 2013, **52**, 4160.
16 L. Cheng, J. Liu, X. Gu, H. Gong, X. Shi, T. Liu, C. Wang, X. Wang, G. Liu, H. Xing, W. Bu, B. Sun and Z. Liu, *Adv. Mater.*, 2014, **26**, 1886.
17 W. Yin, L. Yan, J. Yu, G. Tian, L. Zhou, X. Zheng, X. Zhang, Y. Yong, J. Li, Z. Gu and Y. Zhao, *ACS Nano*, 2014, **8**, 6922.
18 K. Kim, J. H. Ryu, D. Y. Lee and H. Lee, *Biomater. Sci.*, 2013, **1**, 783.
19 X. Gu, Y. Zhang, H. Sun, X. Song, C. Fu and P. Dong, *J. Nanomater.*, 2015, **2015**, 1.
20 Y. Liu, K. Ai, J. Liu, M. Deng, Y. He and L. Lu, *Adv. Mater.*, 2013, **25**, 1353.
21 Y. Li, W. Lu, Q. Huang, C. Li and W. Chen, *Nanomedicine*, 2010, **5**, 1161.
22 Q. Tian, M. Tang, Y. Sun, R. Zou, Z. Chen, M. Zhu, S. Yang, J. Wang, J. Wang and J. Hu, *Adv. Mater.*, 2011, **23**, 3542.
23 M. Zhou, R. Zhang, M. Huang, W. Lu, S. Song, M. P. Melancon, M. Tian, D. Liang and C. Li, *J. Am. Chem. Soc.*, 2010, **132**, 15351.
24 R. M. B. O. Duarte, E. B. H. Santos and A. C. Duarte, *Water Res.*, 2003, **37**, 4073.
25 J.-L. Chen, X.-P. Yan, K. Meng and S.-F. Wang, *Anal. Chem.*, 2011, **83**, 8787.
26 M. Bláha, M. Varga, J. Prokeš, A. Zhigunov and J. Vohlídal, *Eur. Polym. J.*, 2013, **49**, 3904.
27 K. Dong, Z. Liu, Z. Li, J. Ren and X. Qu, *Adv. Mater.*, 2013, **25**, 4452.
28 M. Lin, C. Guo, J. Li, D. Zhou, K. Liu, X. Zhang, T. Xu, H. Zhang, L. Wang and B. Yang, *ACS Appl. Mater. Interfaces*, 2014, **6**, 5860.
29 T. Murakami, K. Ajima, J. Miyawaki, M. Yudasaka, S. Iijima and K. Shiba, *Mol. Pharmaceutics*, 2004, **1**, 399.
30 A. Choucair, P. Lim Soo and A. Eisenberg, *Langmuir*, 2005, **21**, 9308.
31 Z. Zhang, L. Wang, J. Wang, X. Jiang, X. Li, Z. Hu, Y. Ji, X. Wu and C. Chen, *Adv. Mater.*, 2012, **24**, 1418.

Nanoscale Accepted Manuscript

This journal is © The Royal Society of Chemistry 20xx